Proceedings of the 2011 IEEE
International Conference on Robotics and Biomimetics
December 7-11, 2011, Phuket, Thailand

3-D Command State-Based Modifiable Walking of a Humanoid Robot on Uneven Terrain with Different Inclinations and Heights

Young-Dae Hong and Jong-Hwan Kim

Abstract— **This paper proposes 3-D command state (3-D CS)-based modifiable walking pattern generator (MWPG) on the uneven terrain with the different inclinations and heights for humanoid robots. In the previous researches on walking pattern generation on the uneven terrain, the humanoid robot was unable to modify a walking pattern on the uneven terrain without any additional footstep for adjusting the center of mass (COM) motion. Thus, a novel MWPG is developed to solve this problem. It is based on the conventional MWPG which allows the zero moment point (ZMP) variation in real-time by closed form functions. Initially, a 3-D CS is defined as a navigational command set which consists of the foot height and foot pitch and roll angles of the swing leg in addition to the single and double support times and sagittal and lateral step lengths of the swing leg, for walking on the uneven terrain. Next, the COM trajectories in the single and double support phases are generated to satisfy the 3-D CS. Also, the foot trajectory of the swing leg is generated according to the commanded sagittal and lateral step lengths, foot height, and foot pitch and roll angles to walk on the uneven terrain. The proposed algorithm is implemented on a simulation model of the small-sized humanoid robot, HanSaRam-IX (HSR-IX), developed at the Robot Intelligence Technology laboratory, KAIST and the effectiveness is demonstrated through the simulation.**

I. INTRODUCTION

A humanoid robot is one of the representative research topics in the robotics society. Various humanoid robots have been developed [1]–[3] and also many studies on the walking pattern generator for stable walking have been carried out [4]–[6]. Meanwhile, most of walking pattern generators have been developed on the assumption that the terrain is flat. However, in real environment, there exist not only flat but also uneven terrains. Therefore, the development of the walking pattern generator on the uneven terrain is one of the essential research issues for the humanoid robots.

Kajita and Tani modeled a humanoid robot as a linear inverted pendulum model (LIPM) to generate a walking pattern on the uneven terrain [7]. Huang *et al.* introduced a walking control consisting of a feedforward dynamic pattern and a feedback sensory reflex which includes a zero moment point (ZMP) reflex, landing-phase reflex, and body-posture reflex [8]. Kajita *et al.* presented a walking pattern generator based on the preview controller [9], which allows an auxiliary ZMP control [10]. Nishiwaki *et al.* provided a posture control using an attitude measurement sensor and a center of pressure control [11]. Takubo *et al.* presented a method to modify the landing timing and landing position of the swing leg by the ZMP criteria map [12]. There were approaches to generate the walking pattern on the uneven terrain using the contact wrench sum as a stability criterion [13]–[15]. Ohashi *et al.* presented an environment mode which is transformed from a sensor information [16]. It represented contact states between the terrain and soles. Kang *et al.* developed a foot mechanism using an optical distance sensor to detect the terrain height [17]. Aoyama *et al.* modeled the humanoid robot as a special 3-D LIPM that could change the length [18]. The 3-D LIPM was modeled as a 2-D autonomous system by applying the passive dynamic autonomous control based on the assumption of point-contact [19].

This paper proposes 3-D command state (3-D CS)-based modifiable walking pattern generator (MWPG) on the uneven terrain with the different inclinations and heights for humanoid robots. In the previous researches on walking pattern generation on the uneven terrain, the humanoid robot was unable to modify a walking pattern during the single support phase. Consequently, it was impossible to independently change the walking pattern, i.e. single and double support times, sagittal and lateral step lengths, foot height, and foot pitch and roll angles of the swing leg on the uneven terrain without any additional footstep for adjusting the center of mass (COM) motion. Thus, a novel MWPG is developed to solve this problem. It is based on the conventional MWPG which allows the ZMP variation in real-time by closed form functions [5], [6]. The conventional MWPG can be applied only on the flat terrain. However, the proposed MWPG is able to independently modify the walking pattern on the uneven terrain with the different inclinations and heights. Initially, a 3-D CS is defined as a navigational command set which consists of the foot height and foot pitch and roll angles of the swing leg in addition to the single and double support times and sagittal and lateral step lengths of the swing leg, for walking on the uneven terrain. Next, the COM trajectories in the single and double support phases are generated to satisfy the 3-D CS. In the single support phase, the primary dynamics of the humanoid robot is modeled as a 3-D LIPM, the COM height of which is constant, and the dynamic equation of the 3-D LIPM is derived to obtain the sagittal and lateral COM motions with two ZMP functions. Using the sagittal and lateral COM motions, the sagittal and lateral COM trajectories in the single support phase are generated to satisfy the sagittal and lateral step lengths and the foot pitch and roll angles of the swing leg. In the double support phase, the vertical COM trajectory is generated to satisfy the foot height of the swing leg from the single support phase. Also, the foot trajectory of the swing leg is generated according to the commanded sagittal

The authors are with the Department of Electrical Engineering, KAIST, 335 Gwahak-ro, Yuseong-gu, Daejeon 305-701, Republic of Korea (e-mail: {ydhong, johkim}@rit.kaist.ac.kr).

978-1-4577-2138-0/11/$26.00 © 2011 IEEE

and lateral step lengths, foot height, and foot pitch and roll angles to walk on the uneven terrain. The proposed algorithm is implemented on a simulation model of the small-sized humanoid robot, HanSaRam-IX (HSR-IX), developed at the Robot Intelligence Technology laboratory, KAIST and the effectiveness is demonstrated through the simulation.

This paper is organized as follows. Section II presents the definition and determination method of the 3-D CS. In Section III, the 3-D CS-based MWPG on the uneven terrain with the different inclinations and heights is proposed. The COM trajectory generation in the single and double support phases is described and the foot trajectory generation of the swing leg is also explained. In Section IV, the simulation result is presented and finally conclusions follow in Section V.

II. 3-D COMMAND STATE

A. Definition

As a navigational command set, the conventional CS is insufficient because the terrain is uneven in the real environment [5], [6]. Particularly, the terrain has different inclinations and heights. Thus, the foot height and foot pitch and roll angles of the swing leg should be considered in the CS to generate the walking pattern on the uneven terrain. In this paper, the 3-D CS is defined as a novel navigational command set as follows:

***Definition** 1:* 3-D command state (3-D CS) is defined as

$$\textbf{3-D CS} \equiv [T^{ss}_{l/r} \;\; T^{ds}_{l/r} \;\; S_{l/r} \;\; L_{l/r} \;\; H_{l/r} \;\; \phi_{l/r} \;\; \psi_{l/r}]$$

where

$T^{ss}_{l/r}$: single support time during left/right support phase;
$T^{ds}_{l/r}$: double support time from left/right support phase to right/left support phase;
$S_{l/r}$: sagittal step length of left/right leg;
$L_{l/r}$: lateral step length of left/right leg;
$H_{l/r}$: foot height of left/right leg;
$\phi_{l/r}$: foot pitch angle of left/right leg;
$\psi_{l/r}$: foot roll angle of left/right leg.

B. Determination of the 3-D CS

Fig. 1 shows the walking on the uneven terrain, in which there exists a board with the different inclination and height compared to the flat terrain. The solid-line rectangle and small circle represent the boundary and the position of the foot, respectively. f_l, f_r, f_f, and f_b denote the distances from the foot position to each boundary, respectively. o_l and o_w denote the length and width from the foot position to the nearest point of the board, respectively and o_h denotes the height of the board at the point. ϕ_o and ψ_o denote the pitch and roll angles of the board, respectively. If ϕ_o is positive/negative, the board is inclined upward/downward. Similarly, if ψ_o is positive/negative, the board is inclined leftside/rightside. In this paper, it is assumed that the information about the terrain could be obtained using the embedded sensors and the 3-D CS is determined according to the information as follows:

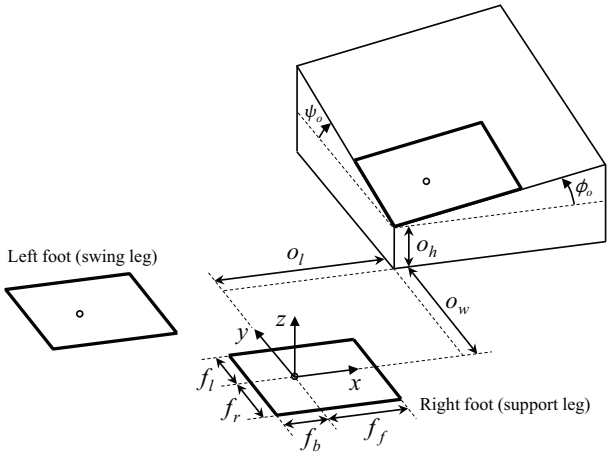

Fig. 1. Walking on uneven terrain with the different inclination and height. The solid-line rectangle and small circle represent the boundary and the position of the foot, respectively.

$$S_{l/r} = o_l + f_b \cos\phi_o \quad (1)$$
$$L_{l/r} = o_w \pm f_{r/l} \cos\psi_o \quad (2)$$
$$H_{l/r} = o_h + f_b \sin\phi_o \pm f_{r/l} \sin\psi_o \quad (3)$$
$$\phi_{l/r} = \phi_o \quad (4)$$
$$\psi_{l/r} = \psi_o. \quad (5)$$

III. 3-D CS BASED-MWPG ON UNEVEN TERRAIN WITH DIFFERENT INCLINATIONS AND HEIGHTS

The walking of the humanoid robot is composed of single support phase and double support phase, and in the single support phase, the primary dynamics of the humanoid robot on the flat terrain is modeled as a 3-D LIPM [4]. In the 3-D LIPM, it is assumed that the support leg is a weightless telescopic limb and the mass is concentrated as a single point without vertical motion. Consequently, it is possible to decouple the sagittal and lateral motion equations. To walk on the uneven terrain with the different inclinations and heights, in this paper, the 3-D LIPM is extended to the walking on the inclined board in both pitch and roll directions.

A. COM Trajectory Generation in Single Support Phase

Fig. 2 shows the 3-D LIPM on the inclined board in both pitch and roll directions. By applying the Newton-Euler formulation, the dynamic equation of the 3-D LIPM for the angular momentum taken around the contact point between the pendulum model and ground surface in the frame $\{R\}$ is obtained as follows:

$$\mathbf{T}_{gr} + \mathbf{r}_{com} \times \mathbf{F}_{gr} = \frac{d}{dt}(\mathbf{r}_{com} \times \mathbf{L}) \quad (6)$$

where $\mathbf{T}_{gr} = [T_x \; T_y \; T_z]^T$ denotes the torque created by the ground reaction force (GRF), $\mathbf{r}_{com} = [x \; y \; z]^T$ denotes the vector from the contact point to the COM, and $\mathbf{L}$ denotes the linear momentum of the COM. Gravitational force $\mathbf{F}_{gr}$

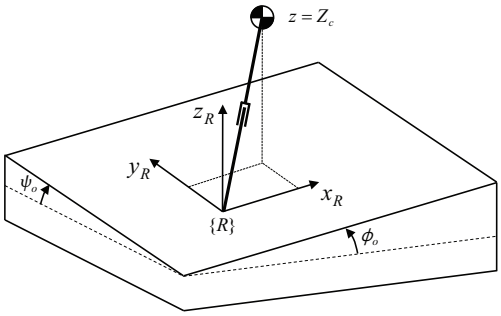

Fig. 2. 3-D LIPM on inclined board in pitch and roll directions.

is given as

$$\mathbf{F}_{gr} = \begin{bmatrix} -mgS_{\phi_o} \\ -mgS_{\psi_o} \\ -mgC_{\phi_o}C_{\psi_o} \end{bmatrix} \tag{7}$$

where m is the mass of the pendulum. S_θ and C_θ denote $\sin\theta$ and $\cos\theta$, respectively. Since the height of the COM, z is constant Z_c, (6) can be rewritten as follows:

$$\begin{bmatrix} \ddot{y} - \frac{gC_{\phi_o}C_{\psi_o}}{Z_c}y + gS_{\psi_o} \\ \ddot{x} - \frac{gC_{\phi_o}C_{\psi_o}}{Z_c}x + gS_{\phi_o} \end{bmatrix} = \begin{bmatrix} -\frac{T_x}{mZ_c} \\ \frac{T_y}{mZ_c} \end{bmatrix}. \tag{8}$$

The ZMP is used to represent the sum of the torques caused by the GRF as follows:

$$\mathbf{T}_{gr} - \mathbf{r}_{zmp} \times \mathbf{F}_{gr} = \begin{bmatrix} 0 & 0 & M_z \end{bmatrix}^T \tag{9}$$

where $\mathbf{r}_{zmp} = [x_{zmp} \;\; y_{zmp} \;\; 0]^T$ and M_z denote the ZMP and the yaw moment, respectively. T_x and T_y are obtained from (9), and then the following dynamic equation of the 3-D LIPM can be obtained by substituting them into (8):

$$\begin{bmatrix} \ddot{y} - \frac{gC_{\phi_o}C_{\psi_o}}{Z_c}y + gS_{\psi_o} \\ \ddot{x} - \frac{gC_{\phi_o}C_{\psi_o}}{Z_c}x + gS_{\phi_o} \end{bmatrix} = -\frac{gC_{\phi_o}C_{\psi_o}}{Z_c}\begin{bmatrix} y_{zmp} \\ x_{zmp} \end{bmatrix}. \tag{10}$$

The above equation provides the relationship between the ZMP and the sagittal and lateral COM motions of the 3-D LIPM on the inclined board in both pitch and roll directions.

The solutions of (10), which mean the sagittal and lateral COM motions of the 3-D LIPM on the inclined board, are obtained by applying the inverse Laplace transform as follows:

Sagittal COM motion:

$$\begin{aligned} \begin{bmatrix} x_f \\ v_f T_c \end{bmatrix} &= \begin{bmatrix} Ch_T & Sh_T \\ Sh_T & Ch_T \end{bmatrix}\begin{bmatrix} x_i \\ v_i T_c \end{bmatrix} - \frac{1}{T_c}\begin{bmatrix} \int_0^T Sh_T\bar{p}(t)dt \\ \int_0^T Ch_T\bar{p}(t)dt \end{bmatrix} \\ &\quad + \begin{bmatrix} -gT_c^2 S_{\phi_o}(-1+Ch_T) \\ -gT_c^2 S_{\phi_o} Sh_T \end{bmatrix} \end{aligned} \tag{11}$$

Lateral COM motion:

$$\begin{aligned} \begin{bmatrix} y_f \\ w_f T_c \end{bmatrix} &= \begin{bmatrix} Ch_T & Sh_T \\ Sh_T & Ch_T \end{bmatrix}\begin{bmatrix} y_i \\ w_i T_c \end{bmatrix} - \frac{1}{T_c}\begin{bmatrix} \int_0^T Sh_T\bar{q}(t)dt \\ \int_0^T Ch_T\bar{q}(t)dt \end{bmatrix} \\ &\quad + \begin{bmatrix} -gT_c^2 S_{\psi_o}(-1+Ch_T) \\ -gT_c^2 S_{\psi_o} Sh_T \end{bmatrix} \end{aligned} \tag{12}$$

with

$$T_c = \sqrt{\frac{Z_c}{gC_\phi C_\psi}}.$$

$(x_i, v_i)/(x_f, v_f)$ and $(y_i, w_i)/(y_f, w_f)$ denote initial/final COM position and velocity in sagittal and lateral planes, respectively. Sh_T and Ch_T are defined as $\sinh(T/T_c)$ and $\cosh(T/T_c)$, respectively. T is the remaining single support time, and $p(t)$ and $q(t)$ are ZMP functions for the sagittal and lateral COM motions, respectively, where $\bar{p}(t) = p(T-t)$ and $\bar{q}(t) = q(T-t)$. $p(t)$ and $q(t)$ are selected by the constant and step functions, respectively as follows [5]:

$$p(t) = \begin{cases} P, & \text{if } 0 \le t < T \\ 0, & \text{otherwise} \end{cases}, \; q(t) = \begin{cases} Q, & \text{if } 0 \le t < T_{sw} \\ -Q, & \text{if } T_{sw} \le t \le T \end{cases} \tag{13}$$

where P and Q are the magnitudes of the constant and step functions, respectively. T_{sw} is the switching time of the step function.

The first terms on the right-hand side of (11) and (12) are homogeneous solutions of (10). The second terms are the particular solutions that make the sagittal and lateral COM motions more extensive by varying the ZMP trajectories with $p(t)$ and $q(t)$. In the conventional 3-D LIPM [4], it was assumed that the ZMP was fixed at a contact point, thus the particular solutions were not considered. Consequently, in the single support phase, the sagittal and lateral COM motions of the 3-D LIPM are predetermined and unmodifiable. Namely, the humanoid robot is unable to independently modify the walking pattern, i.e. single and double support times, sagittal and lateral step lengths, foot height, and foot pitch and roll angles of the swing leg in the conventional 3-D LIPM. However, in the MWPG, since the COM position and velocity can be changed independently at any time during the single support phase by the ZMP functions $p(t)$ and $q(t)$ in real-time, the MWPG enables the humanoid robot to modify the walking pattern independently by the ZMP variation without any additional footstep for adjusting the COM motion. The last terms perform shifting the COM trajectory of the 3D-LIPM for walking on the inclined board according to the pitch and roll angles of the board (ϕ_o and ψ_o). In addition, the MWPG effectively reduces computational cost since the closed form functions are used for the ZMP variation, which ensures a real-time calculation.

Using the above sagittal and lateral COM motions (11) and (12), the sagittal and lateral COM trajectories in the single support phase are generated to satisfy the sagittal and lateral step lengths and the foot pitch and roll angles of the swing leg. The COM position and velocity in the sagittal and lateral planes are defined as a walking state (WS) of the 3-D LIPM and the WS is derived for the commanded CS [5], [6]. Then, the sagittal and lateral COM trajectories satisfying the WS are generated by (11) and (12).

B. COM Trajectory Generation in Double Support Phase

As mentioned above, the vertical COM motion is not considered to decouple the sagittal and lateral COM motion

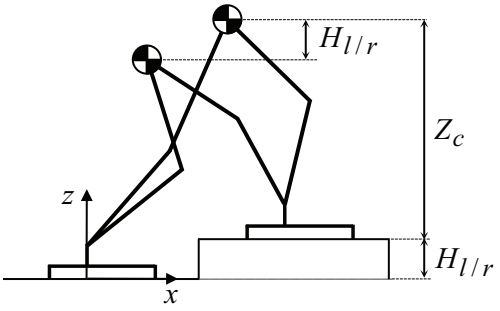

Fig. 3. Vertical COM motion in double support phase.

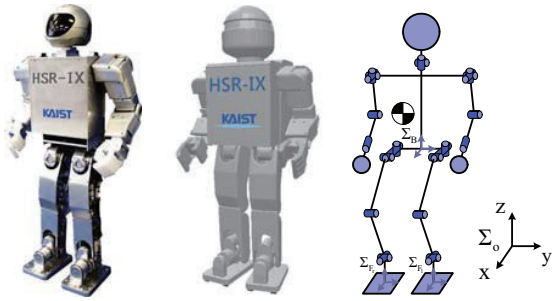

(a) (b) (c)

Fig. 4. (a) HSR-IX. (b) Simulation model. (c) Configuration.

equations in the conventional MWPG [5], [6]. In this paper, however, the vertical COM trajectory in the double support phase is generated to satisfy the foot height of the swing leg from the single support phase, $H_{l/r}$ instead of using the constant COM height. As shown in Fig. 3, the COM height maintains the constant Z_c during the single support phase, and then it moves to $Z_c + H_{l/r}$ during the double support phase by the cubic spline interpolation with Z_c at $t = 0$ and $Z_c + H_{l/r}$ at $t = T^{ds}_{l/r}$ as follows:

$$z(t) = -2\frac{H_{l/r}}{T^{ds\,3}_{l/r}}t^3 + 3\frac{H_{l/r}}{T^{ds\,2}_{l/r}}t^2 + Z_c. \tag{14}$$

Note that the vertical COM trajectory is defined with respect to the local coordinate frame attached on the support leg. In the double support phase, the sagittal and lateral COM motions travel with constant velocity.

C. Foot Trajectory Generation of Swing Leg

The sagittal and lateral foot trajectories of the swing leg, $(x_{foot},\ y_{foot})$ are generated by the cubic spline interpolation with the sagittal and lateral step lengths at the previous footstep, $(-S^{pre}_{r/l},\ -L^{pre}_{r/l})$ at $t = 0$ and $(S_{l/r},\ L_{l/r})$ at $t = T^{ss}_{l/r}$ as follows:

$$x_{foot}(t) = -2\frac{S_{l/r} + S^{pre}_{r/l}}{T^{ss\,3}_{l/r}}t^3 + 3\frac{S_{l/r} + S^{pre}_{r/l}}{T^{ss\,2}_{l/r}}t^2 - S^{pre}_{r/l} \tag{15}$$

$$y_{foot}(t) = -2\frac{L_{l/r} + L^{pre}_{r/l}}{T^{ss\,3}_{l/r}}t^3 + 3\frac{L_{l/r} + L^{pre}_{r/l}}{T^{ss\,2}_{l/r}}t^2 - L^{pre}_{r/l}. \tag{16}$$

The vertical foot trajectory of the swing leg, z_{foot} is generated by a cycloid function. In order to satisfy the commanded foot height $H_{l/r}$, the trajectory Δz_{foot} is supplied, which is generated by the cubic spline interpolation with the foot height of the swing leg at the previous footstep, $-H^{pre}_{r/l}$ at $t = 0$ and $H_{l/r}$ at $t = T^{ss}_{l/r}$ as follows:

$$z_{foot}(t) = r\left(1 - cos\left(\frac{2\pi t}{T^{ss}_{l/r}}\right)\right) + \Delta z_{foot}(t) \tag{17}$$

with

$$\Delta z_{foot}(t) = -2\frac{H_{l/r} + H^{pre}_{r/l}}{T^{ss\,3}_{l/r}}t^3 + 3\frac{H_{l/r} + H^{pre}_{r/l}}{T^{ss\,2}_{l/r}}t^2 - H^{pre}_{r/l}$$

where r denotes the radius of the cycloid circle. The foot pitch and roll angle trajectories of the swing leg, $(\phi_{foot},\ \psi_{foot})$ are generated by the cubic spline interpolation with the foot pitch and roll angles of the swing leg at the previous footstep, $(-\phi^{pre}_{r/l},\ -\psi^{pre}_{r/l})$ at $t = 0$ and $(\phi_{l/r},\ \psi_{l/r})$ at $t = T^{ss}_{l/r}$ as follows:

$$\phi_{foot}(t) = -2\frac{\phi_{l/r} + \phi^{pre}_{r/l}}{T^{ss\,3}_{l/r}}t^3 + 3\frac{\phi_{l/r} + \phi^{pre}_{r/l}}{T^{ss\,2}_{l/r}}t^2 - \phi^{pre}_{r/l} \tag{18}$$

$$\psi_{foot}(t) = -2\frac{\psi_{l/r} + \psi^{pre}_{r/l}}{T^{ss\,3}_{l/r}}t^3 + 3\frac{\psi_{l/r} + \psi^{pre}_{r/l}}{T^{ss\,2}_{l/r}}t^2 - \psi^{pre}_{r/l}. \tag{19}$$

IV. SIMULATION

The proposed algorithm was implemented on the simulation model of the small-sized humanoid robot, HSR-IX in Fig. 4. HSR has been in continual development and research by the Robot Intelligence Technology laboratory, KAIST [6]. Its height and weight are 52.8 cm and 5.5 kg, respectively. It has 26 DOFs which consist of 12 DC motors with harmonic drives in the lower body and 16 RC servo motors in the upper body (two servo motors in each hand control). The on-board Pentium-III compatible PC, running RT-Linux, calculates the proposed algorithm every 5 msec in real-time.

The simulation model of HSR-IX was modeled by Webot, which is the 3-D robotics simulation software and enables users to conduct the physical and dynamical simulation [20], as shown in Fig. 4(b). The COM height Z_c was set as 22.2 cm. In the simulation environment, there were five boards with different inclinations and heights as shown in Table I and the 3-D CS list for the simulation was determined by (5) according to the information about the terrain. Table II shows the commanded 3-D CS list, in which sagittal and lateral step lengths, foot height, and foot pitch and roll angles of the swing leg were independently changed while maintaining the same walking period at each footstep for walking on the uneven terrain.

Fig 5 shows the snapshots of the walking simulation result. As the figure shows, HSR-IX walked stably on the uneven terrain with the different inclinations and heights by

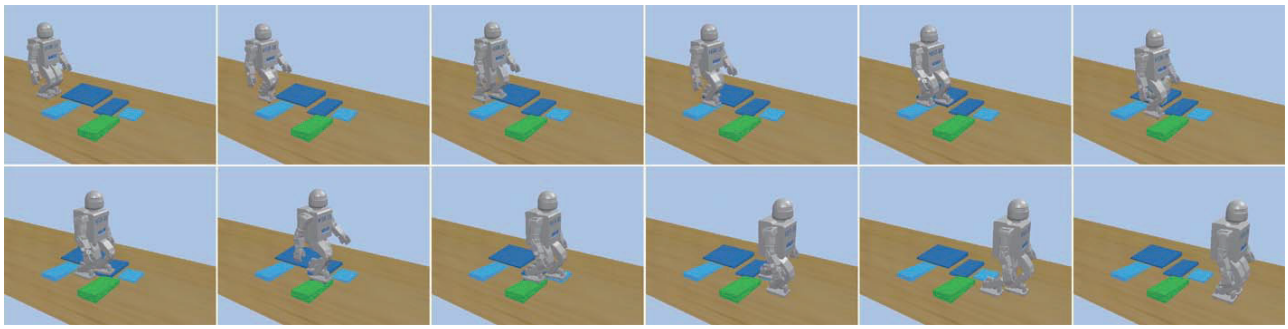

Fig. 5. Snapshots of the walking simulation result (left to right, top to bottom).

TABLE I

INCLINATIONS AND HEIGHTS OF THE BOARDS (LENGTH AND ANGLE UNITS WERE GIVEN IN CENTIMETERS AND DEGREES, RESPECTIVELY.)

	board 1	board 2	board 3	board 4	board 5
ϕ_o	0.0	0.0	5.0	5.0	5.0
ψ_o	5.0	-5.0	0.0	-5.0	5.0
o_h	1.0	0.5	1.0	1.5	0.5

TABLE II

COMMANDED 3-D CS LIST (TIME, LENGTH, AND ANGLE UNITS WERE GIVEN IN SECONDS, CENTIMETERS AND DEGREES, RESPECTIVELY.)

Steps	$T^{ss}_{l/r}$	$T^{ds}_{l/r}$	$S_{l/r}$	$L_{l/r}$	$H_{l/r}$	$\phi_{l/r}$	$\psi_{l/r}$
1^{st} (right foot)	0.80	0.40	7.00	-6.00	0.00	0.00	0.00
2^{nd} (left foot)	0.80	0.40	7.00	6.00	1.27	0.00	5.00
3^{rd} (right foot)	0.80	0.40	7.00	-6.00	-0.50	0.00	-5.00
4^{th} (left foot)	0.80	0.40	7.00	6.00	0.50	0.00	5.00
5^{th} (right foot)	0.80	0.40	7.00	-10.00	-1.27	0.00	0.00
6^{th} (left foot)	0.80	0.40	7.00	6.00	1.26	5.00	0.00
7^{th} (right foot)	0.80	0.40	8.00	-6.00	0.77	5.00	-5.00
8^{th} (left foot)	0.80	0.40	7.00	9.00	-0.70	5.00	5.00
9^{th} (right foot)	0.80	0.40	11.00	-8.00	-0.84	0.00	0.00
10^{th} (left foot)	0.80	0.40	9.50	6.00	0.00	0.00	0.00
11^{th} (left foot)	0.80	0.40	0.00	-6.00	0.00	0.00	0.00

modifying the sagittal and lateral step lengths, foot height, and foot pitch and roll angles of the swing leg according to the commanded CS list at every footstep. Fig. 6 shows the generated COM trajectories with respect to the global coordinate frame attached on the terrain. As shown in the figure, in the single support phases, the sagittal and lateral COM trajectories were generated to satisfy the sagittal and lateral step lengths and foot pitch and roll angles of the swing leg in CS list by (11) and (12), and the vertical COM trajectory maintained the constant value. In the double support phases, the vertical COM trajectory was generated to satisfy the foot heights of the swing leg from the single support phases by (14). In addition, the foot trajectories of the swing leg were generated by (15), (16), (17), (18) and (19). Fig. 7 shows the measured ZMP trajectories in the walking simulation. It can be seen that the ZMP trajectories in the x-axis and y-axis followed the foot trajectories with a little variation. The little variation of the ZMP trajectories was mainly due to the dynamic difference between HSR-IX and the 3D-LIPM. However, the ZMP trajectories were within the upper and lower boundaries of foot trajectories, which means that HSR-IX could walk on the uneven terrain with the different inclinations and heights while maintaining stability.

V. CONCLUSION

In this paper, 3-D CS-based MWPG on the uneven terrain with the different inclinations and heights for humanoid robots was proposed. The effectiveness of the proposed algorithm was verified through the simulation for the simulation model of the small-sized humanoid robot, HSR-IX. As a novel navigational command set, the 3-D CS was defined by adding the foot height and foot pitch and roll angles of the swing leg to the conventional CS and it was given according to the information about the terrain. Then, the COM trajectories in the single and double support phases were generated to satisfy the 3-D CS, also the foot trajectory of the swing leg was generated to walk on the uneven terrain. Consequently, by using the proposed algorithm, the humanoid robot could walk stably on the uneven terrain with the different inclinations and heights following the commanded 3-D CS list by modifying the sagittal and lateral step lengths, foot height, and foot pitch and roll angles of the swing leg at every footstep.

VI. ACKNOWLEDGMENTS

This research was supported by Basic Science Research Program through the National Research Foundation of Korea (NRF) funded by the Ministry of Education, Science and Technology (2011-0000321).

REFERENCES

[1] Y. Sakagami, R. Watanabe, C. Aoyama, S. Matsunaga, N. Higaki, and K. Fujimura, "The intelligent ASIMO: system overview and integration," in *Proc. IEEE/RSJ Int. Conf. Intell. Robot. Syst.*, 2002, pp. 2478–2483.

[2] K. Akachi, K. Kaneko, N. Kanehira, S. Ota, G. Miyamori, M. Hirata, S. Kajita, and F. Kanehiro, "Development of humanoid robot HRP-3P," in *Proc. IEEE-RAS Int. Conf. Humanoid Robots*, 2005, pp. 50–55.

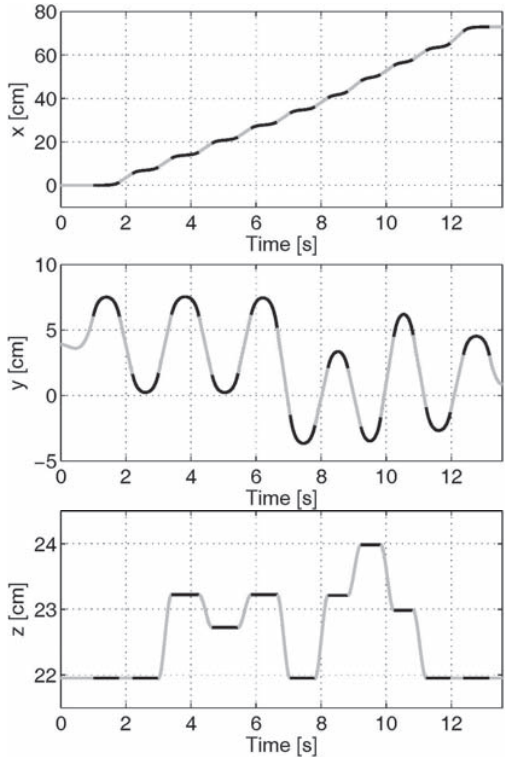

Fig. 6. Generated sagittal, lateral and vertical COM trajectories with respect to the global coordinate frame attached on the terrain. The thick and thin lines represent the COM trajectories in the single and double support phases, respectively.

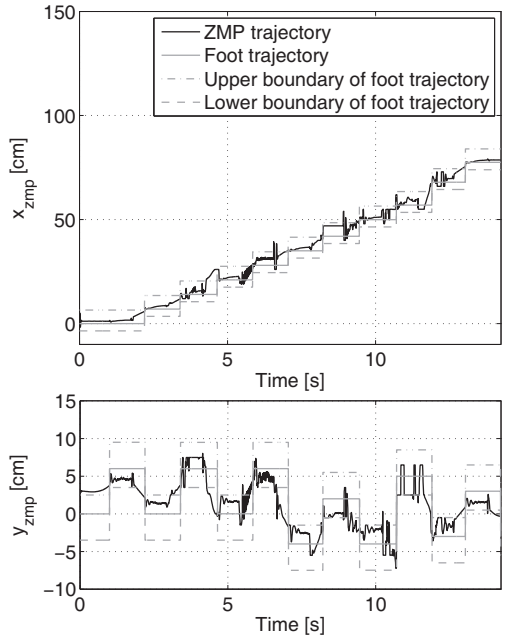

Fig. 7. Measured ZMP trajectories in the walking simulation.

[3] Y. Ogura, H. Aikawa, K. Shimomura, H. Kondo, A. Morishima, H.-O. Lim, and A. Takanishi, "Development of a new humanoid robot WABIAN-2," in *Proc. IEEE Int. Conf. Robot. Autom.*, 2006, pp. 76–81.

[4] S. Kajita, F. Kanehiro, K. Kaneko, K. Fujiwara, K. Yokoi, and H. Hirukawa, "A realtime pattern generator for biped walking," in *Proc. IEEE Int. Conf. Robot. Autom.*, 2002, vol. 1, pp. 31–37.

[5] B.-J. Lee, D. Stonier, Y.-D. Kim, J.-K. Yoo, and J.-H. Kim, "Modifiable walking pattern of a humanoid robot by using allowable ZMP variation," *IEEE Trans. Robot.*, vol. 24, no. 4, pp. 917–925, 2008.

[6] Y.-D. Hong, B.-J. Lee, and J.-H. Kim, "Command state-based modifiable walking pattern generation on an inclined plane in pitch and roll directions for humanoid robots," *IEEE/ASME Trans. Mechatron.*, vol. 16, no. 4, pp. 783–789, 2011.

[7] S. Kajita and K. Tani, "Study of dynamic biped locomotion on rugged terrain -Derivation and application of the linear inverted pendulum mode-," in *Proc. IEEE Int. Conf. Robot. Autom.*, 1991, pp. 1405–1411.

[8] Q. Huang and Y. Nakamura, "Sensory reflex control for humanoid walking," *IEEE Trans. Robot.*, vol. 21, no. 5, pp. 977–984, 2005.

[9] S. Kajita, F. Kanehiro, K. Kaneko, K. Fujiwara, K. Harada, K. Yokoi, and H. Hirukawa, "Biped walking pattern generation by using preview control of zero-moment point," in *Proc. IEEE Int. Conf. Robot. Autom.*, 2003, vol. 2, pp. 1620–1626.

[10] S. Kajita, M. Morisawa, K. Harada, K. Kaneko, F. Kanehiro, K. Fujiwara, and H. Hirukawa, "Biped walking pattern generator allowing auxiliary ZMP control," in *Proc. IEEE/RSJ Int. Conf. Intell. Robot. Syst.*, 2006, pp. 2993–2999

[11] K. Nishiwaki and S. Kagami, "Walking control on uneven terrain with short cycle pattern generation," in *Proc. IEEE-RAS Int. Conf. Humanoid Robots*, 2007, pp. 447–453.

[12] T. Takubo, Y. Imada, K. Ohara, Y. Mae, and T. Arai, "Rough terrain walking for bipedal robot by using ZMP criteria map," in *Proc. IEEE Int. Conf. Robot. Autom.*, 2009, pp. 788–793.

[13] H. Hirukawa, S. Hattori, K. Harada, S. Kajita, K. Kaneko, F. Kanehiro, K. Fujiwara, and M. Morisawa, "A universal stability criterion of the foot contact of legged robots - adios ZMP," in *Proc. IEEE Int. Conf. Robot. Autom.*, 2006, pp. 1976–1983.

[14] H. Hirukawa, S. Hattori, S. Kajita, K. Harada, K. Kaneko, F. Kanehiro, M. Morisawa, and S. Nakaoka, "A pattern generator of humanoid robots walking on a rough terrain," in *Proc. IEEE Int. Conf. Robot. Autom.*, 2007, pp. 2181–2187.

[15] Y. Zheng, M. C. Lin, D. Manocha, A. H. Adiwahono, and C.-M. Chew, "A walking pattern generator for biped robots on uneven terrains," in *Proc. IEEE/RSJ Int. Conf. Intell. Robot. Syst.*, 2010, pp. 4483–4488.

[16] E. Ohashi, T. Sato, and K. Ohnishi, "A walking stabilization method based environmental modes on each foot for biped robot," *IEEE Trans. Ind. Electron.*, vol. 56, no. 10, pp. 3964–3974, 2009.

[17] H.-J. Kang, K. Hashimoto, H. Kondo, K. Hattori, K. Nishikawa, Y. Hama, H.-O. Lim, A. Takanishi, K. Suga, and K. Kato, "Realization of biped walking on uneven terrain by new foot mechanism capable of detecting ground surface," in *Proc. IEEE Int. Conf. Robot. Autom.*, 2010, pp. 5167–5172.

[18] T. Aoyama, K. Sekiyama, Y. Hasegawa, and T. Fukuda, "3-D biped walking over rough terrain based on the assumption of point-contact," in *Proc. IEEE/RSJ Int. Conf. Intell. Robot. Syst.*, 2010, pp. 3163–3168

[19] M. Doi, Y. Hasegawa, and T. Fukuda, "Passive dynamic autonomous control of bipedal walking," in *Proc. IEEE-RAS Int. Conf. Humanoid Robots*, 2004, pp. 811–829.

[20] O. Michel, "Cyberbotics Ltd. WebotsTM: Professional mobile robot simulation," *Int. J. Adv. Robot. Syst.*, vol. 1, no. 1, pp. 39–42, 2004.